Low Cycle Fatigue Properties of Extruded 6061-T6 Aluminum Alloy

IOP Conf. Series: Journal of Physics: Conf. Series **1198** (2019) 032002 doi:10.1088/1742-6596/1198/3/032002

Low Cycle Fatigue Properties of Extruded 6061-T6 Aluminum Alloy

M Badaruddin [a], Zulhanif , H Supriadi

Department of Mechanical Engineering, Faculty of Engineering, Universitas Lampung Jalan Prof. S. Brojonegoro No. 1 Bandar Lampung 35145, Indonesia

[a] Corresponding author: mbruddin@eng.unila.ac.id

Abstract. This paper presents the low cycle fatigue properties of an extruded 6061 aluminum alloy. The cyclic strain-controlled fatigue tests were performed under fully reversed total strain amplitudes ranging from 0.5% to 1.3% at a fixed strain rate of 0.004 s^{-1} using smooth specimens cyclically loaded along with the extrusion directions. The fatigue test results represented by the hysteresis curves of stress-strain show slight Bauschinger effect at the total strain amplitudes ($\Delta\varepsilon_{at}$) ≤ 0.7 %. The corresponding cyclic strain response revealed that the alloy underwent cyclic softening particularly at the lower strain amplitude ($\Delta\varepsilon_{at}$ ≤0.7%) and at the higher strain amplitudes, the alloy tended to undergo cyclic hardening. The strain-fatigue life models were empirically determined by the Coffin-Manson-Basquin relationships.

1. Introduction

Recently, the aerospace, and automotive industries have been developing lightweight-alloy designs in order to increase efficiency in fossil fuel consumption use. Alternatively, an aluminium (Al) 6061 alloy has been chosen as a structural component because the alloy has high strength and ductility, good machinability, resistance to corrosion, good weldability, and good abrasion resistance [1, 2]. The Al-6061 alloy is an Al silicon magnesium alloy that has good strength and very high formability; therefore, the alloy can be manufactured via an extrusion process into complex geometries such as multi-hollow bodies [3, 4]. This makes the 6061 Al alloy very adaptable for use in plates, extrusions, foils, sheets, pipes, forgings, and even structural forms in the aerospace, construction, and transportation industries [5]. The structural engineering of the 6061 alloy involves cyclic loading due to the fact that structural components in a vehicle subject to fluctuating load over elastic strain region, thus leading to higher plastic deformation that results in the occurrence of low cycle fatigue (LCF) failure [6]. Hence, an understanding of LCF properties of the 6061-T6 alloy is essential for the design and analysis of engineering components.

A review of literature regarding fatigue in 6061 aluminum alloys reveals some experimental studies that have characterized fatigue behavior based on load-control cyclic tests or high cycle fatigue [4,5,7–9]. However, for applications in which LCF is dominant within variable-strain amplitude histories, strain-controlled fatigue tests are better than stress-controlled fatigue tests for characterizing fatigue behavior. However, few data sets concerning the 6061 aluminum alloy's strain-controlled fatigue are available in the literature; for example, one data set was published in conference proceedings [6] and the other was published in a journal [10]. Mirza et al. [6] conducted the low cycle fatigue test of the extruded 6061-T6 aluminum alloy using the highest possible strain amplitude (1.2%) and a strain rate of 0.01 s^{-1}. Furthermore, similar tests were conducted by Brammer et al. [10]

using a fixed frequency of 5 Hz under conditions of different strain amplitudes. Existing low-cycle fatigue properties of the 6061-T6 aluminum alloy describes the fatigue life of the alloy, which is significantly affected by strain amplitude, rate, and frequency. Therefore, the purpose of the present study was to determine low cycle fatigue properties of an extruded 6061-T6 aluminum alloy under various higher strain amplitudes ranging from 0.5% to 1.3% at a strain rate of 0.004 s^{-1}. The present results were compared with the results reported by Mirza et al. [6] and Brammer et al. [10].

2. Experimental procedure

A commercially extruded 6061-T6 Al alloy in a round bar with 20 mm in diameter and 150 mm in length was machined using a CNC EMCO machine lathe for providing tensile and low cycle fatigue (LCF) specimens according to the international testing standards, ASTM B557 [11] and ASTM E606, respectively [12]. The diameter and the total gauge length of the tensile specimens were 6 and 40 mm, respectively. LCF specimens had a diameter of 6.35 mm with a total gage length of 30 mm. Prior to testing, all specimens were hand-ground in the loading direction with 800-grit silicon carbide paper to remove residual stress and any machine marks. Tensile tests were performed using a computerized MTS Landmark 100 kN servo-hydraulic testing system with an axial extensometer gauge length of 10 mm (Model: 632.13F-20 MTS) under control of a strain rate of 0.5% min^{-1} from starting test to yield point determination and later control of a displacement rate of 0.25 mm min^{-1} until specimen failure. The LCF tests were conducted using MTS Landmark 100 kN operated by Multipurpose LCF template. The cyclic loading tests consisted of a strain ratio of R = −1, a constant strain rate, ($\dot{\varepsilon}$) of 0.004 s^{-1}, and a total strain amplitude ($\Delta\varepsilon_{at}$) of 0.5, 0.7, 1.1, and 1.3% under a triangular loading waveform. In this study, crack initiation cycle and cycles to failure (N_f) were defined as the number of cycles at which the maximum tensile load range decreased by 10% and 25% from that in a stable and saturated region, respectively.

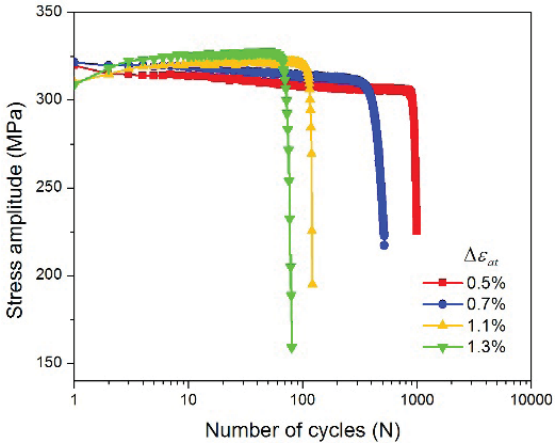

Figure 1. Cyclic stress amplitude versus number of cycles at different total strain amplitudes of extruded 6061-T6 aluminum (Al) alloy.

3. Results and discussion

3.1. Cyclic stress response

Plot of stress amplitudes with respect to the number of cycles at different strain amplitudes ranging from 0.5 to 1.3% is displayed in Fig 1 under a semi-logarithmic scale along the X- axis. It can be observed that the cyclic stress amplitude increases with an increase in total strain amplitude, whereas the fatigue life of the extruded 6061-T6 Al alloy decreased with increasing total strain amplitudes. During the low cycle fatigue of the 6061-T6 Al alloy, the total of the plastic strain amplitude can be

considered as the amount of physical quantity that is generated by dynamically obstructing dislocation movements as result of coupling effects between internal microstructures and particle phase magnesium silicide (Mg_2Si) precipitates [7]. Typical stress-strain hysteresis loops of the first stable crack initiation and failure cycles at total strain amplitudes of 0.7% and 1.3% are displayed in Figs. 2a and b, respectively. The tensile and compressive stress resulting from cyclic loading during the first cycle was slightly higher than the tensile and compressive stress resulting from a stable cycle that could lead to the alloy's softening behaviour (Fig. 2a). In addition, the current 6061-T6 Al alloy was also observed to exhibit unsymmetrical hysteresis loops with only a slight downward shift in compression (Fig. 2a) at the first cycle until it reached stable cycles. This phenomenon was similar to most of the face-centered cubic metals that result from an obstacle dislocation movement that can generate plastic deformation in most ductile materials [13]. It can be clearly seen in Fig 2a that slight unsymmetrical compressive stress tips generate a phenomenon in the alloy that distinguishes it as the Bauschinger-like effect [14]. When the alloy experiences a loading in the compressive direction, the dislocations resulted are not able to inhibit the reversed stresses, thus leading to small dislocation annihilation. Consequently, additional cycles generate initial alloy softening of the alloy. As shown in Fig. 2b, the Bauschinger effect was not found in the alloy during low cycle fatigue tests with the highest strain amplitude of 0.7% during those tests. Fig. 2b shows the cyclic loading, during which the higher strain amplitude generates a larger size of the alloy's hysteresis loop, which indicates a larger portion of plastic region.

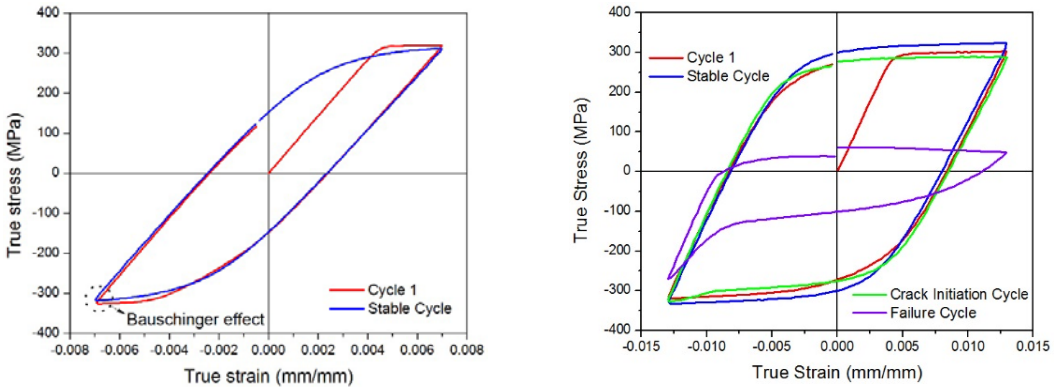

Figure 2. Typical stress–strain hysteresis loops of different cycles of the extruded 6061-T6 Al alloy tested at $= 0.004\ s^{-1}$ and total strain amplitudes of (a) 0.7% and (b) 1.3 %.

Fig. 3a shows cyclic softening within the half of the cycle failure that was at the strain amplitudes of 0.5% to 0.7%; these findings are in contrast to the results reported for the extruded 6061-T6 Al alloy as described by Ref. [6,10]. It indicates that at the lower strain amplitude of 0.7%, the extruded 6061-T6 Al alloy tends toward softening behavior in which the secondary phase particles (Mg_2Si) in the alloy are not able to retain dislocation movement, thus leading to dislocation annihilation until the alloy fails. Furthermore, at strain amplitudes >0.7%, the alloy undergoes initial strain hardening with increasing strain amplitudes (Fig. 3a). With strain amplitudes ranging from 1.1% to 1.3%, the cyclic hardening experienced by the alloy can be attributed to interactions between the presence of small size secondary phase particles and Mg_2Si-precipitates that obstruct the dislocation movement [15].

The variations in strain amplitude that correspond to failure cycle reversal is shown in Fig. 4a and to changes in stress amplitude during cyclic deformation is shown in Fig. 3b at different total strain amplitudes. As shown in Fig. 2b, as the higher strain amplitudes caused an increase in the plastic strain amplitudes, but consequently, the fatigue life of the alloy was decreased. As noted for

monotonic loading, the extruded aluminum alloy showed lower stress responses under cyclic loading at strain amplitudes <1.1% as shown in Fig. 3b.

In addition, cyclic plastic deformation is defined as the portion of the plastic strain amplitude in which the elastic strain amplitude is independent. The relationship of stress amplitude to plastic strain can be expressed by Equation (1):

$$\sigma_a = K'(\epsilon_{ap})^{n'} \quad (1)$$

in which $\Delta\sigma_a$ and $\Delta\varepsilon_{ap}$ are the stress amplitudes and plastic strain amplitudes at half-life cycles, respectively. n' is the cyclic strain-hardening exponent, and K' is the cyclic strength coefficient that was obtained using curve fitting by plotting a double log-$\Delta\sigma_a$ versus $\Delta\varepsilon_{ap}$ curve.

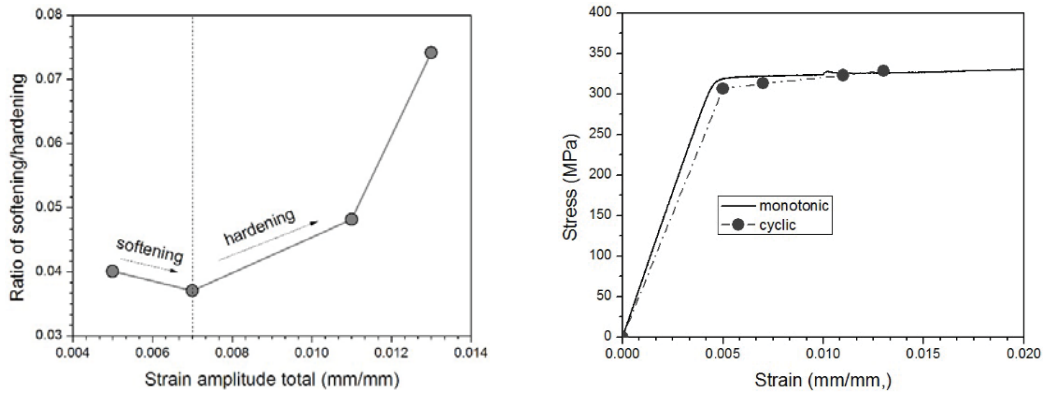

(a) (b)

Figure 3. (a) Effect of strain amplitude on the cyclic softening and hardening, (b) Stress–strain curve of extruded 6061-T6 Al alloy.

3.2. Low cycle fatigue properties

Fig. 4a presents the total strain amplitude $\Delta\varepsilon_t$ as a function of the number of cycles to failure (N_f, fatigue life) for the extruded 6061-T6 Al alloy. The alloy showed a trend toward increasing fatigue life with decreasing strain amplitude, and overall, the material generally showed an improved fatigue life compared to extruded 6061-T6 Al alloys reported in the literature [6,10]. This phenomenon is closely related to material strength and ductility. In addition, the alloy undergoes higher ductility and lower strength (Fig. 3b), which leads to better fatigue resistance at lower strain amplitudes.

The low cycle fatigue properties of the extruded 6061-T6 Al alloy were determined by the Basquin-Coffin-Manson relationship in form of Equation (2):

$$\Delta\varepsilon_t = \Delta\varepsilon_{ae} + \Delta\varepsilon_{ap} = \frac{\sigma_f'}{E}(2N_f)^b + \varepsilon_f'(2N_f)^c \quad (2)$$

in which E is Young's modulus (for the present material, the average value obtained during fatigue testing was ~68.94 GPa), N_f is the fatigue life or the number of cycles to failure, σ_f'(MPa) is the fatigue strength coefficient, b is the fatigue strength exponent, ϵ_f' is the fatigue ductility coefficient, and c is the fatigue ductility exponent.

Fig. 4a displays the elastic, plastic, and total strain amplitudes as a function of the number of reversals to failure ($2N_f$). In addition, the empirical models that are based on the Basquin-Coffin-Manson's equation approach show good correlation with the test data as shown in Fig. 4a. In order to ensure that cyclic stabilization, also called cyclic saturation, had already occurred in the alloy, the stress amplitude and plastic strain amplitude values at the half-life cycles were used (Fig. 4b). Hence, the fatigue life parameters obtained by means of Equations (1) and (2) are presented in Table 1, which

show the comparisons between the resulting strain-life properties from this study and the strain-life properties determined in previous studies described in the literature.

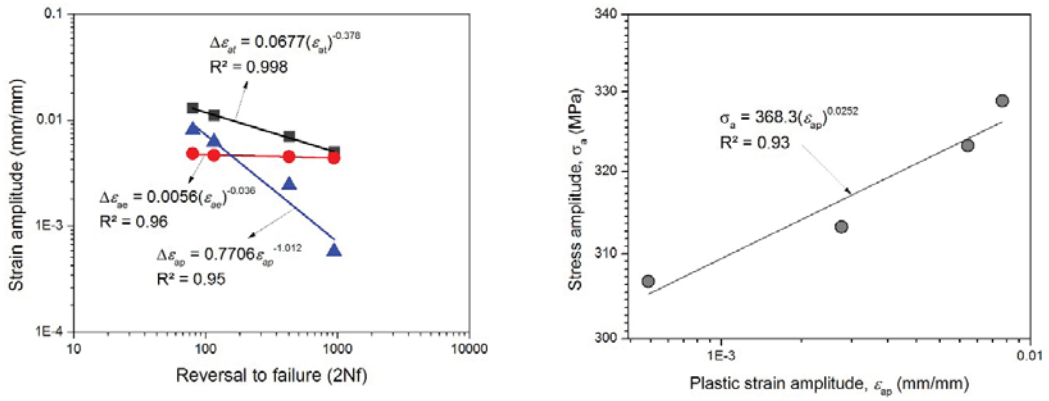

(a) (b)

Figure 4. (a) A typical strain amplitude-failure cycle curve and (b) plastic strain–stress relationship curve of the extruded 6061-T6 Al alloy.

These results show that the LCF parameters determined using Equation (2) show significant differences in cyclic strength and fatigue strength coefficients, cyclic strain hardening, and fatigue ductility coefficient values with the values reported by Brammer et al. [10]. However, the cyclic strength coefficients and the fatigue ductility exponents (*K'* and c, respectively) are almost identical with the values reported by Mirza et al. [6] in their previous study. These differences in the Coffin-Manson approach suggest that there is slightly more plastic strain effect above a 1.1% strain amplitude in the extruded material. However, it can be seen that the resulting fatigue parameters were well within the range of both studies' values. Both the *K′* value and *n′* were obtained from plot of double logarithmic stress versus strain amplitude (Fig. 4b). The resulting cyclic strain hardening exponent (*n′* = 0.025) of the present 6061-T6 Al alloy was higher than the corresponding monotonic strain hardening exponent (*n* = 0.017) as can be seen in Table 1. This could be the main reason why this alloy exhibited cyclic hardening even at the higher strain amplitude of 1.1%. The comparison of LCF parameters from the present research with studies described in the literature [6,10] are displayed in Table 1.

Table 1. Low cycle fatigue parameters of the extruded 6061-T6 Al alloy

LCF Parameters	Extruded 6061-T6 aluminum alloy		
	Present study	Ref. [6]	Ref. [10]
Cyclic strength coefficient, *K′*	368	369	268
Fatigue strength coefficient, σ_f', MPa	386	534	705
Cyclic strain hardening exponent, *n′*	0.025	0.039	0.078
Fatigue strength exponent, *b*	−0.036	−0.08	−0.11
Fatigue ductility coefficient, ϵ_f', mm/mm	0.77	4.49	2.40
Fatigue ductility exponent, *c*	−1.01	−1.10	−0.98

Conclusion

Strain-controlled fatigue tests were conducted on an extruded 6061 Al alloy with various strain amplitudes at strain rate of 0.004 s^{-1}. The stress–strain responses mostly exhibited unsymmetrical responses as a consequence of the obstacle dislocation slip-dominated plastic deformation with Bauschinger effect. The alloy experiences softening behavior at strain amplitudes ≤0.7%. At strain amplitudes >0.7%, the alloy has started to experience cyclic hardening until it reaches cyclic

stabilization and failure. It indicates that from the corresponding cyclic stress response during fatigue loading revealed that cyclic hardening particularly occurred at a higher strain amplitude of 0.7%. The low cycle fatigue parameters of the presently described extruded 6061-T6 Al alloy were observed to be significantly different compared with the other previously described extruded 6061 Al alloys resulting from the fact that the behavior of the alloy's low cycle fatigue is significantly affected by both strain amplitude and rate. In addition, the strain-life models determined by adequately approaching the Basquin-Coffin-Manson relationship show good correlation with strain-controlled fatigue test data.

Acknowledgments
The authors would like to thank the Ministry Research, Technology and Higher Education of Republic of Indonesia, through the Fundamental Research grant in fiscal year of 2017-2018.

References
1. Okayasu M, Ohkura Y, Takeuchi S, Takasu S, Ohfuji H and Shiraishi T 2012 *Mater. Sci. Eng. A* **543** 185.
2. Ammar HR, Samuel AM and Samuel FH 2008 *Intl. J. Fat.* **30** 1024.
3. Fan KL, He GQ, Liu XS, Liu B, She M, Yuan YL, Yang Y and Lu Q 2013 *Mater. Sci. Eng. A* **586** 78.
4. Takahashi Y, Yoshitake H, Nakamichi R, Wada T, Takuma M, Shikama T and Noguchi H 2014 *Mater. Sci. Eng. A* **614** 243.
5. Takahashi Y, Shikama T, Nakamichi R, Kawata Y, Kasagi N, Nishioka H, Kita S, Takuma M and Noguchi H 2015 *Mater. Sci. Eng. A* **641** 263.
6. Mirza FA, Liu K and Chen XG 2017 Cyclic stress-strain behavior and low cycle fatigue life of AA6061 aluminum alloy. In: Ratvik AP (ed.) Light Metals 2017. The Minerals, Metals & Materials Series. Springer, pp. 447–452.
7. Takahashi Y, Shikama T, Yoshihara S, Aiura T and Noguchi H 2012 *Acta Mater.* **60** 2554.
8. Li WA, Li ZY, Shuai H, Xiao SH, and Yong Z 2017 *Intl. J. Fat*. **95** 216.
9. Odeshi AG, Adesola AO and Badmos AY 2013 *Eng. Fail Anal.* **35** 302.
10. Brammer AT, Jordon JB, Allison PG and Barkey ME 2013 *J. Mater. Eng. Perform*. **22** 1348.
11. ASTM B557-15 Standard test methods for tension testing wrought and cast aluminum- and magnesium-alloy Products, ASTM International, West Conshohocken, PA, 2015.
12. ASTM E 606-04 Standard practice for strain-controlled fatigue testing, ASTM International, West Conshohocken, PA, 2004.
13. Jordon JB, Horstemeyer MF, Solanki K and Xue Y 2007 *Mech. Mater*. **39** 920.
14. Zuhair MG and Syed SA 2013 *Mater. Sci. Eng. A* **562** 109.
15. Kumar N, Goel S, Jayaganthan R and Owolabi GM 2018 *Intl. J. Fat*. **110** 130.